

# Magnetocaloric effect in pyrochlore antiferromagnet $\text{Gd}_2\text{Ti}_2\text{O}_7$

S. S. Sosin, L. A. Prozorova, A. I. Smirnov

*P. L. Kapitza Institute for Physical Problems RAS, 119334 Moscow, Russia*

A. I. Golov, I. B. Berkutov\*

*Department of Physics and Astronomy, University of Manchester, Manchester M13 9PL, UK*

O. A. Petrenko, G. Balakrishnan

*Department of Physics, University of Warwick, Coventry CV4 7AL, UK*

M. E. Zhitomirsky

*Commissariat à l'Energie Atomique, DSM/DRFMC/SPSMS, Grenoble Cédex 9, France*

(Dated: April 22, 2004)

An adiabatic demagnetization process is studied in the pyrochlore antiferromagnet  $\text{Gd}_2\text{Ti}_2\text{O}_7$ . By decreasing magnetic field we observe a cooling of the sample up to 10 times in the field range from 120 to 50 kOe corresponding to a crossover between saturated and spin-liquid phases. This phenomenon indicates that a considerable part of the magnetic entropy associated with a macroscopic number of local soft modes survives in the strongly correlated paramagnetic state. Monte Carlo simulations demonstrate good agreement with the experiment. The cooling power of the process is experimentally estimated with a view to possible technical applications. The results on  $\text{Gd}_2\text{Ti}_2\text{O}_7$  are compared to those for  $\text{Gd}_3\text{Ga}_5\text{O}_{12}$ , a standard material for low temperature magnetic cooling.

PACS numbers: 75.30.Sg, 75.50.Ee, 75.30.Kz.

The distinct feature of highly frustrated magnetic materials is a peculiar spatial arrangement of the magnetic ions. Nearest-neighbor antiferromagnets on typical geometrically frustrated structures, like, for instance, kagome, garnet, and pyrochlore lattices, have an infinite number of classical ground states. A macroscopic degeneracy precludes any type of conventional magnetic ordering. As a result, frustrated magnets remain in a disordered cooperative paramagnetic ground state at temperatures well below the paramagnetic Curie-Weiss constant  $\theta_{CW}$  [1]. Weak residual interactions, or quantum and thermal fluctuations usually induce some kind of ordered or spin-glass state at  $T^* \ll \theta_{CW}$ . A number of geometrically frustrated magnets have been experimentally studied in the past decade [2]. Magnetic pyrochlore compound  $\text{Gd}_2\text{Ti}_2\text{O}_7$  is one of the prototype examples. The  $\text{Gd}^{3+}$  ions have  $S = 7/2$  and zero orbital momentum, which yields a good realization of a nearest-neighbor Heisenberg exchange antiferromagnet on a pyrochlore lattice. Recent specific heat, susceptibility and neutron scattering measurements [3, 4, 5] have shown that  $\text{Gd}_2\text{Ti}_2\text{O}_7$  remains disordered over a wide temperature interval below the Curie-Weiss constant  $\theta_{CW} \simeq 10$  K. The transition to an ordered phase is presumably driven by weak dipole-dipole interactions and occurs only at  $T_{N1} \approx 1$  K.

Infinite degeneracy of the magnetic ground state of a frustrated magnet is equivalent to presence of a macroscopic number of local zero-energy modes. Such soft modes correspond to degrees of freedom, which rotate a finite number of spins with no change in the total ex-

change energy. In a pyrochlore structure (a matrix of corner-sharing tetrahedra on the fcc lattice), these groups of spins are hexagons formed by the edges of neighboring tetrahedra, which lie in the kagome planes [(111) and equivalent planes]. In zero applied field, if the six spins are arranged antiferromagnetically around one hexagon, they effectively decouple from the other spins and can rotate by an arbitrary angle. The low-energy hexagon modes have been observed in quasielastic neutron scattering studies on spinel compound  $\text{ZnCr}_2\text{O}_4$  [6], which is a spin-3/2 Heisenberg antiferromagnet on a pyrochlore lattice. The thermodynamic consequence of these local excitations is that a considerable fraction of the magnetic entropy is not frozen down to temperatures much less than  $\theta_{CW}$ .

An interesting effect related to a field evolution of the zero-energy local modes is an enhanced magnetocaloric effect near the saturation field  $H_{\text{sat}}$  predicted recently in [7]. Transformation between a nondegenerate fully polarized spin state above  $H_{\text{sat}}$  and an infinitely degenerate magnetic state below  $H_{\text{sat}}$  occurs via a condensation of a macroscopic number of local modes and produces large variations of entropy in magnetic field. Therefore, an experimental observation of the magnetocaloric effect in  $\text{Gd}_2\text{Ti}_2\text{O}_7$  should be important both from a fundamental point of view, as a physical probe of the local zero-energy excitations in the frustrated ground state below  $H_{\text{sat}}$ , and because of the possible technological applications. The enhanced magnetic cooling power of gadolinium gallium garnet  $\text{Gd}_3\text{Ga}_5\text{O}_{12}$  has been known for a long time [8, 9, 10], although without reference to

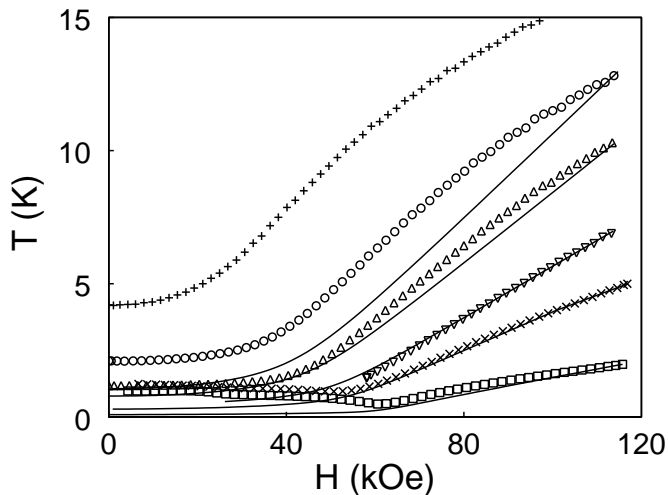


FIG. 1: Temperature variations for the adiabatic demagnetization of  $\text{Gd}_2\text{Ti}_2\text{O}_7$ . Solid lines are obtained by Monte Carlo simulations with the exchange constant  $J = 0.3$  K.

frustrated properties of a garnet (hyper-kagome) lattice. Experiments have been also performed on other garnets [11]. Thus, a comparison between the two typical frustrated magnets is important since a stronger frustration on a pyrochlore lattice produces the maximal cooling rate among geometrically frustrated magnets [7]. In the present work we study experimentally and theoretically the magnetocaloric effect in  $\text{Gd}_2\text{Ti}_2\text{O}_7$ . Demagnetization of a  $\text{Gd}_2\text{Ti}_2\text{O}_7$  sample under quasi-adiabatic conditions is measured and compared to a similar study of  $\text{Gd}_3\text{Ga}_5\text{O}_{12}$ . Classical Monte Carlo simulations of an ideal adiabatic demagnetization process are performed for both materials. Entropy variations and the cooling power of  $\text{Gd}_2\text{Ti}_2\text{O}_7$  in an applied magnetic field are calculated from a combination of the adiabatic demagnetization results and specific heat measurements.

A single-crystal sample of  $\text{Gd}_2\text{Ti}_2\text{O}_7$  was grown by the method described in [12] and is approximately  $3.5 \times 1.5 \times 1$  mm<sup>3</sup> in size (32.5 mg by mass). A commercially available  $\text{RuO}_2$  thermometer with the resistance calibrated down to 100 mK in fields up to 120 kOe was glued onto the sample. It was also used as a heater to regulate the starting temperature of the experiment. The sample was suspended on four thin constantan wires (20  $\mu\text{m}$  in diameter and 5 cm in length) soldered to the thermometer to make a 4-wire resistance measurement. The experimental cell was put in a vacuum chamber immersed in a helium bath held at 1.8–4.2 K. The heat exchange gas inside the chamber was absorbed by a charcoal cryopump to a pressure of  $10^{-7}$  torr. The cryopump was equipped with a heater to desorb some exchange gas when necessary to cool the sample during the experiment. Magnetic fields up to 120 kOe were generated by a cryomagnet. The field  $H$  was applied perpendicular to the  $\langle 111 \rangle$  axis. No correction for the demagnetization factor was made

( $4\pi M$  is always less than  $0.1H$ ).

In the main part of the experiment, the temperature of the sample was measured in a quasi-adiabatic regime as a function of time and magnetic field at a sweep rate of 10 kOe/min. Additionally, a parasitic temperature drift  $\dot{T}_p$  (due to radiation, wiring and the measuring current) was investigated at several fixed values of the field for temperatures along each curve  $T_S(H)$ . The values of  $\dot{T}_p$  have a smooth temperature dependence within the range  $\pm 2$  mK/sec changing sign at about 10 K. The corrected temperature values  $T_{\text{cor}}$  at each field are calculated from measured temperatures by subtracting the parasitic drift integrated to the corresponding point in time:

$$T_{\text{cor}}(H, t_0) = T_{\text{exp}}(H, t_0) - \int_0^{t_0} \dot{T}_p dt \quad (1)$$

The experimental data shown in Fig. 1 are the temperature versus magnetic field records for different starting temperatures. All the curves except the one starting at  $T_i = 2$  K are corrected using Eq. (1). The temperature drop during demagnetization  $T_i/T_f$  depends on the starting temperature. It has a maximum around  $T_i \simeq 10$  K where the temperature drops by a factor of 10. A characteristic feature for all the  $T_S(H)$  curves starting below 10 K is that a significant part of cooling occurs in the field range from 120 to 60 kOe, which contrasts sharply with a continuous adiabatic cooling ( $T/H = \text{constant}$ ) of an ideal paramagnet.

The correction procedure introduced by Eq. (1) is applicable only if the parasitic heating does not strongly affect the whole demagnetization process. A more general heat-balance equation is

$$W_p dt = C dT + T (\partial S / \partial H)_T dH, \quad (2)$$

where  $W_p$  is a parasitic heat leak ( $\dot{T}_p = W_p/C$ ),  $C$  is the specific heat at a constant field. This equation leads to formula (1) if the function  $T(\partial S / \partial H)_T / C \equiv -(\partial T / \partial H)_S$  does not change significantly between  $T_{\text{exp}}$  and  $T_{\text{cor}}$ . Such an assumption is valid for high temperature scans where the correction does not exceed  $0.1T_{\text{exp}}$  while at low  $T$  they are of the same order of magnitude. In addition, the derivative  $(\partial T / \partial H)_S$  strongly decreases in the vicinity of the ordering transition which leads to an overcorrection of the experimental data. This overcorrection is illustrated in Fig. 2 by the dashed line. Thus, an ideal adiabatic dependence  $T_S(H)$  should lie between the raw experimental data and the corrected curve. The minimum temperature reached experimentally on demagnetization from  $T_i = 2$  K at  $H_f = 62$  kOe is  $T_{\text{min}} = 0.48$  K. This cooling limit is associated with the magnetic entropy freezing at the transition into an ordered state. When the field is further decreased, a weak temperature increase is observed. Two temperature plateaus (shown by the arrows in Fig. 2) are clearly seen in this part of the curve corresponding to the phase transitions at  $T_{N_1} \simeq 1$  K and  $T_{N_2} \simeq 0.75$  K [5, 13, 14].

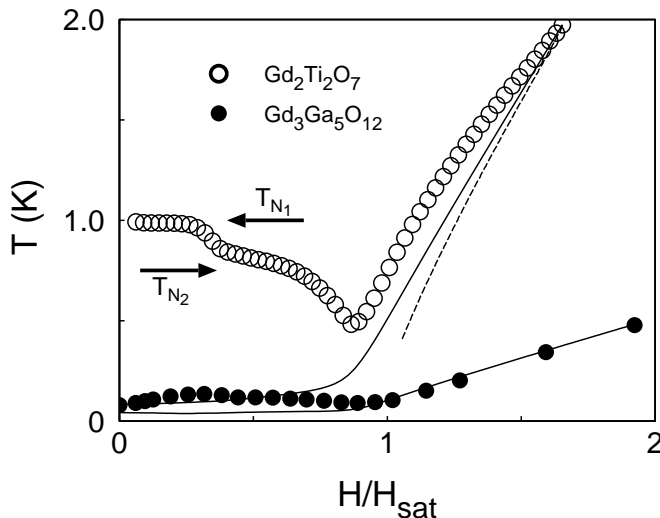


FIG. 2: Comparison of adiabatic demagnetization in  $\text{Gd}_2\text{Ti}_2\text{O}_7$  (raw data) and  $\text{Gd}_3\text{Ga}_5\text{O}_{12}$  on a field scale normalized to  $H_{\text{sat}}$ . Monte Carlo simulations are shown by the solid lines; the dashed line is an overcorrection to the experimental data made using formula (1).

It is interesting to compare the above measurements to the magnetocaloric effect in another frustrated spin system  $\text{Gd}_3\text{Ga}_5\text{O}_{12}$ . These data have been obtained on a sintered powder sample (mass 4.05 g) using an experimental technique similar to that described above. Due to the large heat capacity of the sample no correction for parasitic heat leaks is required in this case. The measured adiabatic demagnetization curves for  $\text{Gd}_3\text{Ga}_5\text{O}_{12}$  are very similar to the previously published results [8], and are compared to  $\text{Gd}_2\text{Ti}_2\text{O}_7$  data in Fig. 2 on a field scale normalized to the corresponding values of  $H_{\text{sat}}$ : 15 kOe and 70 kOe, respectively. The behavior of the  $\text{Gd}_3\text{Ga}_5\text{O}_{12}$  sample is qualitatively similar to what is observed in  $\text{Gd}_2\text{Ti}_2\text{O}_7$ , but occurs in a different temperature range due to a smaller exchange constant. In a demagnetization process of  $\text{Gd}_3\text{Ga}_5\text{O}_{12}$  starting from  $H \simeq 2H_{\text{sat}}$  (28 kOe) at  $T = 0.5$  K the temperature decreases by a factor of 5 reaching its minimum value of 0.1 K in the vicinity of the saturation field after which it remains practically constant.

For a quantitative description of the above experimental data we have performed a series of classical Monte Carlo (MC) simulations using simplified models, which take into account only the nearest-neighbor exchange. A detailed account of the application of the MC technique to model adiabatic processes at constant entropy is given in [7]. Quantum spins  $S = 7/2$  are replaced by classical  $n$ -vectors ( $|\mathbf{n}| = 1$ ), an approximation which is valid for high enough temperatures  $T \gtrsim JS$ . The only parameter required to compare the MC simulations to the experimental data is the exchange constant  $J$ , which is estimated from values of the saturation field or the

Curie-Weiss temperature. Expressions for these quantities for nearest-neighbor antiferromagnets on pyrochlore and garnet lattices are

$$\begin{aligned} g\mu_B H_{\text{sat}} &= 8JS, & k_B\theta_{CW} &= 2JS(S+1), \\ g\mu_B H_{\text{sat}} &= 6JS, & k_B\theta_{CW} &= \frac{4}{3}JS(S+1), \end{aligned} \quad (3)$$

respectively. Corresponding values for both compounds are taken from previous works [3, 5, 13, 15] and are summarized in Table I. For both materials, the exchange constants derived from  $H_{\text{sat}}$  and  $\theta_{CW}$  coincide with an accuracy of  $\sim 10\%$ .

TABLE I: Experimental values  $H_{\text{sat}}$  and  $\theta_{CW}$  and the estimations of the exchange constants for  $\text{Gd}_2\text{Ti}_2\text{O}_7$  and  $\text{Gd}_3\text{Ga}_5\text{O}_{12}$ .

	$H_{\text{sat}}$	$\theta_{CW}$	$J(H_{\text{sat}})$	$J(\theta_{CW})$
$\text{Gd}_2\text{Ti}_2\text{O}_7$	70 kOe	9.5 K	0.33 K	0.30 K
$\text{Gd}_3\text{Ga}_5\text{O}_{12}$	15 kOe	2.3 K	0.1 K	0.11 K

The results of the MC simulations for  $\text{Gd}_2\text{Ti}_2\text{O}_7$  with  $J = 0.3$  K are indicated by the solid lines in Figs. 1 and 2. For the scans starting at temperatures above 10 K the coincidence is rather poor due to a large phonon contribution to the total heat capacity of the sample. The best agreement for this sample is achieved in the intermediate temperature range at fields above  $H_{\text{sat}}$ . Since a nearest-neighbor Heisenberg pyrochlore antiferromagnet does not order, the MC simulations cannot describe properly the observed behavior below  $H_{\text{sat}}$  at  $T < 1$  K. Besides, this is also the limit of the validity of the classical approximation:  $JS \simeq 1$  K. A temperature increase at  $H < H_{\text{sat}}$  observed in  $\text{Gd}_2\text{Ti}_2\text{O}_7$  (Fig. 2) in part results from a parasitic heating but may also be attributed to a reopening of a gap in the excitation spectrum below  $H_{\text{sat}}$  caused by dipolar interactions and other anisotropies. The theoretical dependence obtained for  $\text{Gd}_3\text{Ga}_5\text{O}_{12}$  (lower solid line in Fig. 2) with the exchange constant  $J = 0.11$  K also fits very well the high field part of the experimental adiabatic curve.

Finally, we estimate the cooling power of the demagnetization process using the measured adiabatic  $T_S(H)$  curves along with the specific heat data  $C(T)$  obtained at high fields. The latter measurements were done in a Quantum Design PPMS calorimeter at  $H = 90$  kOe in the temperature range from 1.5 to 20 K. The amount of heat absorbed by a magnetic material during isothermal demagnetization is related to the entropy change  $\Delta Q = T\Delta S|_{H_i}^{H_f}$ . Consider an adiabatic demagnetization curve, which starts at  $(H_i, T_i)$  and ends at  $(H_f, T_f)$ . The entropy along the curve  $T_S(H)$  remains constant, so we can relate the entropy variations at constant temperature and in constant field:

$$\Delta S(T_f)|_{H_i}^{H_f} = \Delta S(H_i)|_{T_f}^{T_i} = \int_{T_f}^{T_i} C(T)/T dT. \quad (4)$$

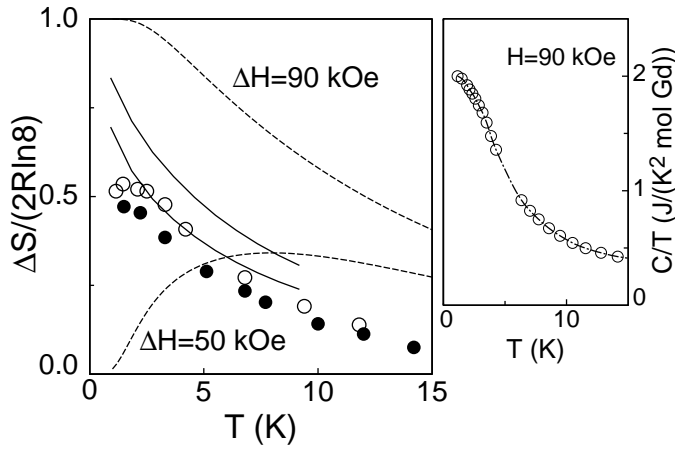


FIG. 3: The molar entropy change of  $\text{Gd}_2\text{Ti}_2\text{O}_7$  under isothermal demagnetization (left panel). Open and closed circles correspond to demagnetization from  $H_i = 90$  kOe to  $H_f = 0$  and from  $H_i = 90$  kOe to  $H_f = 40$  kOe, respectively; solid lines are MC calculations. Entropy variations of an ideal  $S = 7/2$  paramagnet under the same conditions are shown by the dashed lines. Right panel shows the temperature dependence of the specific heat at  $H = 90$  kOe, dashed-dotted line is the spline fit used in the integration in formula (4).

The entropy changes  $\Delta S$  calculated from our experimental data using the above equation are presented in Fig. 3. Two features should be emphasized: (i) about one half of the total magnetic entropy  $2R \ln 8$  remains in the system even at temperatures very close to the transition into an ordered state at  $T_{N_1} = 1$  K; (ii) the largest entropy change  $\Delta S$  and, consequently, a heat absorption  $\Delta Q$  occurs in a high field region above  $H_{\text{sat}}$ . This differs significantly from the behavior of an ideal paramagnet at low temperatures, which releases a significant part of its entropy only if demagnetized to  $H_f \ll H_i$ . Fig. 3 demonstrates that  $\text{Gd}_2\text{Ti}_2\text{O}_7$  has a considerable advantage below 5 K in the *high field* cooling power over conventional paramagnets. For comparison, we show on the same plot similar calculations obtained by the MC simulations of a nearest-neighbor antiferromagnet. Classical models cannot give correct values for the total entropy of a quantum spin system. Nevertheless, the variation of entropy is reproduced with a remarkable accuracy of 10–20%, which is due to the large  $S = 7/2$  spin of the  $\text{Gd}^{3+}$  ions.

The cooling power  $\Delta Q$  has a maximum around 4 K reaching 30 J/mole Gd. Such an amount of heat corresponds, for comparison, to the latent heat of evaporation of approximately 1.5 moles of liquid  $^3\text{He}$  at  $T = 3$  K. The garnet compound  $\text{Gd}_3\text{Ga}_5\text{O}_{12}$  is also advantageous as a refrigerant material over paramagnetic salts, but at lower fields and temperatures. We suggest that a combination of the two compounds might become the basis for a cheap two-stage adiabatic demagnetization refrigerator suitable for effective cooling from  $T \sim 10$  K down to 100

mK range in a single field sweep.

In conclusion, a large magnetocaloric effect is observed in the frustrated pyrochlore antiferromagnet  $\text{Gd}_2\text{Ti}_2\text{O}_7$  in agreement with recent theoretical predictions [7]. This observation points to the presence of a macroscopic number of local low-energy excitations below  $H_{\text{sat}}$ . Such modes can be directly probed in quasielastic neutron scattering measurements analogously to the experiment on  $\text{ZnCr}_2\text{O}_4$  [6]. These excitations may also be responsible for the nonfrozen spin dynamics below  $T_{N_1}$  observed in  $\text{Gd}_2\text{Ti}_2\text{O}_7$  by muon spin relaxation measurements [16]. A comparison between our experimental data and classical MC simulations shows that this numerical technique can semiquantitatively predict the magnetocaloric properties of real rare-earth materials with large (semiclassical) magnetic moments, which were described so far only in the molecular field approximation (see, e.g., [9, 10]).

The authors are indebted to V. I. Marchenko and M. R. Lees for valuable discussions. This work is supported by RFBR grant 04-02-17294 and by the RF President Program. S.S.S. is also grateful to the National Science Support Foundation for the financial help.

---

\* present address: Institute for Low Temperature Physics and Engineering, 47 Lenin avenue, 61103 Kharkov, Ukraine

- [1] J. Villain, Z. Phys. B **33**, 31 (1979); J.T. Chalker, P. Holdworth, E. Shender, Phys. Rev. Lett. **68**, 855 (1992); R. Moessner and J.T. Chalker, *ibid.* **80**, 2929 (1998); B. Canals and C. Lacroix, Phys. Rev. B **61**, 1149 (2000).
- [2] A.P. Ramirez, Geometrical Frustration, in *Handbook of Magnetic Materials* vol. 13, edited by K.H.J. Buschow (Elsevier, Amsterdam, 2001).
- [3] N.P. Raju, *et al.*, Phys. Rev. B **59**, 14 489 (1999).
- [4] J.D.M. Champion *et al.*, Phys. Rev. B **64**, 140407 (2001).
- [5] A.P. Ramirez *et al.*, Phys. Rev. Lett. **89**, 067202 (2002).
- [6] S.-H. Lee *et al.*, Nature **418**, 856 (2002).
- [7] M.E. Zhitomirsky, Phys. Rev. B **67**, 104421 (2003).
- [8] R.A. Fisher *et al.*, J. Chem. Phys. **59**, 4652 (1973); E.W. Hornung *et al.*, *ibid.* **61**, 282 (1974); G.E. Brodale *et al.*, *ibid.* **62**, 4041 (1975).
- [9] J.A. Barclay and W.A. Steyert, Cryogenics **22**, 73 (1982).
- [10] B. Daudin, R. Lagnier, B. Salce, J. Magn. Magn. Mater. **27**, 315 (1982).
- [11] T. Numazawa *et al.*, Physica B **329-333**, 1656 (2003).
- [12] G. Balakrishnan, O.A. Petrenko, M.R. Lees, and D.McK. Paul, J. Phys. Condens. Matter **10**, L723 (1998).
- [13] P. Bonville *et al.*, J. Phys.: Condens. Matter **15**, 7777 (2003).
- [14] O.A. Petrenko *et al.*, cond-mat/0309405.
- [15] W.P. Wolf *et al.*, J. Phys. Soc. Jpn. Suppl. **17**, 443 (1962); S. Hov *et al.*, J. Magn. Magn. Mater. **15-18**, 455 (1980).
- [16] A. Yaouanc *et al.*, Physica B **326**, 456 (2003).